

# Modularity produces small-world networks with dynamical time-scale separation

RAJ KUMAR PAN<sup>(a)</sup> and SITABHRA SINHA<sup>(b)</sup>

*The Institute of Mathematical Sciences, C.I.T. Campus, Taramani, Chennai - 600 113 India*

PACS 89.75.Hc – Networks and genealogical trees  
PACS 05.45.-a – Nonlinear dynamics and chaos  
PACS 89.75.Fb – Structures and organization in complex systems

**Abstract.** - The functional consequences of local and global dynamics can be very different in natural systems. Many such systems have a network description that exhibits strong local clustering as well as high communication efficiency, often termed as small-world networks (SWN). We show that modular organization in otherwise random networks generically give rise to SWN, with a characteristic time-scale separation between fast intra-modular and slow inter-modular processes. The universality of this dynamical signature, that distinguishes modular networks from earlier models of SWN, is demonstrated by processes as different as spin-ordering, synchronization and diffusion.

In many natural situations, dynamics at the local level may occur at a very different time-scale compared to processes taking place on the global level. Such temporal separation is often desirable functionally, e.g., for information processing in the brain, which requires synchrony between local areas processing specific stimuli [1] but where global or very large scale synchrony is considered pathological as in epilepsy [2]. Many systems in nature have network descriptions, with the connection topology playing a crucial role in determining their dynamical behavior [3]. Therefore, it is of considerable interest to understand how the structural organization in complex networks can give rise to dynamics at multiple discrete time-scales.

A large class of networks in nature have been reported to be small-world networks (SWN) [4], which are characterized by the coexistence of very high clustering among neighboring nodes and low average path length. The clustered structure of SWN distinguishes them from networks with “small-world property” [5], whose average path length increases slower than any polynomial function of the system size, a feature seen in random graphs as well as most complex networks [6]. SWN have been reported in a variety of contexts, including the brain [7–9], human society [10] and cellular metabolism [11,12]. Several models for SWN have been proposed [13], beginning with a

simple interpolation scheme between regular and random structure through rewiring of links (the WS model) [4] [Fig. 1(a)]. This creates a few long-range links that act as “shortcuts” between otherwise distant nodes, substantially decreasing the average path length of the graph.

In this paper, we relate the apparently independent properties of dynamical time-scale separation and the clustered small-world property of many complex networks, with the crucial observation that such systems often manifest modular structure [14]. Modules are defined as sub-networks comprising of nodes connected to each other with a density significantly higher than that of the entire network. Modular structures have been observed in a wide variety of contexts, from cellular metabolism [15] and signalling [16] to social communities [17], internet [18] and foodwebs [19]. We use a simple model of modular networks that exhibits all the structural characteristics of SWN, to explore the dynamical consequences of modularity. Such modular networks, in sharp contrast to previous models of SWN, exhibit distinct time-scale separation in their dynamics, corresponding to fast intra-modular and slow inter-modular processes. We show the universality of this behavior by using three very different types of dynamics, viz., (i) the ordering of spins through exchange interactions, (ii) synchronization among strongly nonlinear relaxation oscillators and (iii) diffusion. In all cases, the modular configuration allows coordination within local clusters to occur much more rapidly than global ordering.

<sup>(a)</sup>E-mail: rajkp@imsc.res.in

<sup>(b)</sup>E-mail: sitabhra@imsc.res.in

The occurrence of multiple discrete time-scales in such a wide variety of systems highlights the role of modularity in the dynamics on complex networks. Using this dynamical signature it should also be possible to identify those real-world systems whose SWN property is a consequence of their modular organization. This is crucial for designing intelligent intervention strategies for complex systems, e.g., controlling epidemics.

The network model considered in this paper follows directly from the definition of modular networks and consists of  $N$  nodes arranged into  $m$  modules (similar to the construction used, e.g., in Ref [20]). Each module contains the same number of randomly connected nodes [Fig. 1(b)]. The connection probability between nodes in a module is  $\rho_i$ , and that between different modules is  $\rho_o$ . The parameter defining the model is the ratio of inter- to intra-modular connectivity,  $\frac{\rho_o}{\rho_i} = r \in [0, 1]$ . For  $r \rightarrow 0$ , the network gets fragmented into isolated clusters, while as  $r \rightarrow 1$ , the network approaches a homogeneous or Erdos-Renyi (ER) random network.

We observe that such modular organization gives rise to SWN whose structural properties are very similar to those of networks generated by WS and related models. These properties include the communication efficiency of the network, defined as  $E \equiv \frac{1}{\frac{1}{2}N(N-1)} \sum_{i>j} \frac{1}{d_{ij}}$ , which measures the speed of information propagation over the network [21]. Here,  $d_{ij}$  is the shortest distance between nodes  $i$  and  $j$ . For small  $r$ , as most links are within a module,  $E$  is low, while at large  $r$ ,  $E$  becomes high when the number of inter-modular links increases. We have also measured the clustering within local neighborhoods,  $C = (1/N) \sum_i 2n_i/k_i(k_i - 1)$ , where  $k_i$  and  $n_i$  are the degree and number of links between the neighbors of node  $i$ , respectively. For modular networks with large  $m$ , clustering is high at low  $r$  and decreases with increasing  $r$ . The SWN property, viz., the coexistence of high  $E$  and high  $C$ , is observed in the model for an intermediate range of  $r$  [Fig. 1(c)], exactly as seen in the WS model for intermediate rewiring probability  $p$  [Fig. 1(d)].

We also compare between these models by using a measure for network modularity,  $Q \equiv \sum_{s=1}^m \left[ \frac{l_s}{L} - \left( \frac{d_s}{2L} \right)^2 \right]$ , where  $m$  is the number of modules into which the network is partitioned [22],  $L$  is the total number of links, and  $l_s$  and  $d_s$  are the links between nodes and the total degree of all nodes belonging to module  $s$ , respectively. For  $N$  nodes with average degree  $\langle k \rangle$ , the WS model has a maximum  $Q$  value of  $(1-p) \left[ 1 - \sqrt{(\langle k \rangle + 2)/N} \right]$ , and is very high at low  $p$ . Similarly, for modular random networks,  $Q = \frac{(m-1)[N(1-r)-m]}{m[N(1-r+rm)-m]}$ , which also yields very high values at low  $r$ , where  $Q \sim (1-mr)$  [Fig. 1(e)]. This implies that community detection algorithms which use  $Q$  will be unable to differentiate between these two networks. Other methods, such as, the  $k$ -clique percolation cluster technique [23] indicates high local link density relative to the overall connectivity for both the models. Thus, it is

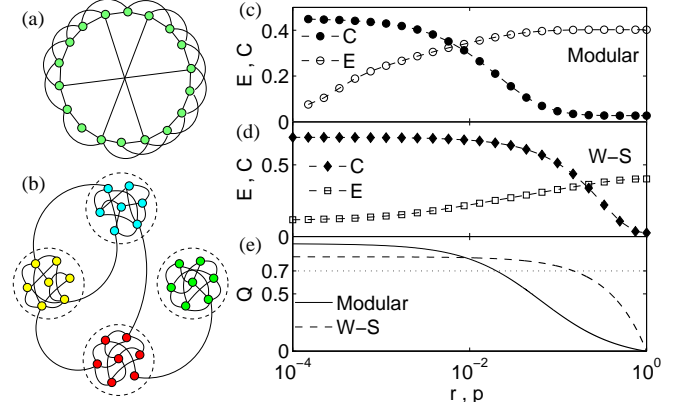


Fig. 1: Schematic diagrams of (a) Watts-Strogatz (WS) model and (b) modular network model (modules indicated by broken curves). Efficiency  $E$  and clustering coefficient  $C$  for (c) modular random network with  $m = 16$  modules as a function of  $r$  and (d) WS model as a function of rewiring probability  $p$  (for all cases  $N = 512$ ,  $\langle k \rangle = 14$ ). Error bars are in all cases smaller than the symbols used. (e) Modularity measure,  $Q$  vs  $r$  for modular random network, and, vs  $p$  for WS network. Intersection of the two curves with the dotted line ( $Q = 0.7$ ) provides  $r, p$  values for comparing the model networks.

difficult to distinguish between WS and modular networks with extant measures that use only structural information.

However, apart from topological structure, networks are often associated with certain dynamics [24]. As dynamics is often crucial for the functioning of many systems, we now examine three very different dynamics on network models having the clustered small-world property. These dynamics range from nonlinear interactions (representative of collective ordering in a network) to strongly nonlinear local dynamics at each node (as in relaxation oscillators) with diffusive coupling. As the WS model is parametrized by  $p$  and the modular random networks by  $r$ , we compare between them by considering networks with the same  $N$ ,  $\langle k \rangle$  and  $Q$ .

We first consider the effect of modular organization on the emergence of collective behavior, a simple model of which is the ordering of Ising spins arranged on a network. This system is described by the Hamiltonian,  $H = -\sum_{i,j} J_{ij} \sigma_i \sigma_j$ , where,  $\sigma_i, \sigma_j = \pm 1$  are spins placed on nodes  $i, j$ , and  $J_{ij}$  is the ferromagnetic coupling between them ( $= J > 0$  if  $i, j$  are connected and 0 otherwise). Starting from an initial random configuration of spins on a modular random network with average degree  $\langle k \rangle$ , the system is allowed to evolve to its ground state using Glauber dynamics. This corresponds to a globally ordered state [Fig 2 (a)] if  $T < T_c (= \langle k \rangle)$ , the mean-field critical temperature measured in units of  $J/k_B$  ( $k_B$ : Boltzmann constant). We observe that the time ( $\tau_{gm}$ ) needed for magnetization  $M = \sum_{i=1}^N \sigma_i / N$  to reach its high asymptotic value, diverges as  $r$  decreases. This is because, at low  $r$ , the system remains for a long time in a

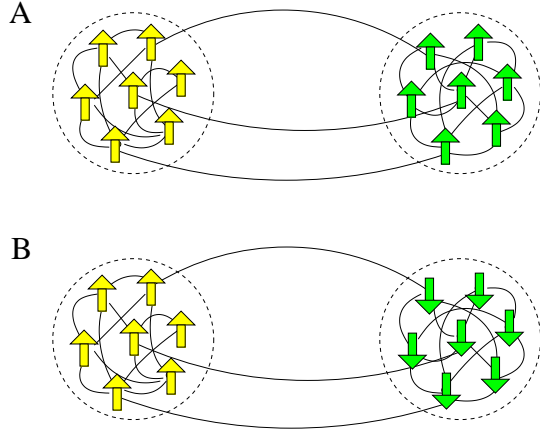


Fig. 2: Schematic diagram of (a) global ordering ( $M = 1$ ,  $M_m = 1$ ) and (b) modular ordering ( $M = 0$ ,  $M_m = 1$ ) in a modular network of Ising spins.

state of modular ordering [Fig 2 (b)], where the spins in each module are ordered but aligned in opposite directions in different modules which results in the absence of global ordering. The local order parameter, modular magnetization  $M_m = (m/N) \langle |\sum_{i \in k} \sigma_i^k| \rangle$ , where  $\sigma_i^k$  is the  $i$ -th spin in the  $k$ -th module and the averaging is over all modules, exhibits convergence to its asymptotic value over a time-scale  $\tau_{mm}$ , which is almost independent of  $r$ . Fig. 3 (a) shows the existence of two time-scales which diverge at low  $r$  indicating the ordering process within modules to be much faster compared to that between modules. At low temperatures, as the spins within each module get ordered, different modules may get aligned in opposite directions. To achieve global order, some of the modules need to turn all their spins, a process that has a considerable energy barrier. To cross this with thermal energy takes extremely long times, resulting in divergence of  $\tau_{gm}$ . A similar investigation of the WS network shows only global ordering, with  $\tau_{gm}$  diverging as  $p$  decreases. Related dynamical processes where the appearance of distinct time-scale events as a consequence of modular network structure have important functional significance, include the adoption of innovations [25], spread of epidemics [26] and consensus formation [27].

Next, we compare the dynamics of synchronization in modular random and WS networks. We consider a population of  $N$  coupled relaxation oscillators (described by a fast variable  $x$  and a slow variable  $y$ ) which evolve as

$$\dot{x}_i = c \left[ y_i - x_i + \frac{x_i^3}{3} \right] + \sum_{j=1}^N \frac{K_{ij}}{k_i} (x_j - x_i); \quad (1)$$

$$\dot{y}_i = \frac{-x_i}{c}. \quad (2)$$

Here,  $c$  is the ratio between time-scales of  $x$  and  $y$ .  $K_{ij} = \kappa A_{ij}$  is the coupling between a connected pair of oscillators with strength  $\kappa$ , and  $\mathbf{A}$  is the network adjacency

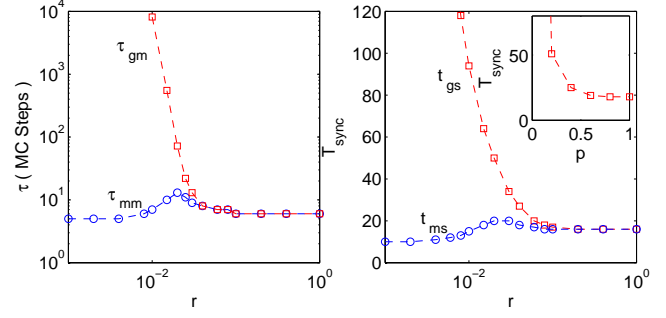


Fig. 3: (a) The two time-scales corresponding to local ordering within a module ( $\tau_{mm}$ ) and global ordering over the entire network ( $\tau_{gm}$ ) for a modular random network of Ising spins ( $m = 16$ ) at  $T = 6$  as a function of  $r$ , showing their divergence at low  $r$ . (b) Comparison of synchronization between modular random networks ( $m = 16$ ) and WS networks of relaxation oscillators (Eqs.1-2) with  $c = 2$  and  $\kappa = 1.5$ . In modular networks, the two time-scales corresponding to intra-modular ( $t_{ms}$ ) and global or inter-modular ( $t_{gs}$ ) synchronization are shown as a function of  $r$ . The WS model exhibits only the time-scale corresponding to global synchronization (inset). Averaging has been done over random initial values and network realizations. (In all cases  $N = 512$ ,  $\langle k \rangle = 14$ ).

matrix, i.e.,  $A_{ij} = 1$  if  $i, j$  are connected and 0 otherwise. The local dynamics of these relaxation oscillators is strongly nonlinear compared to, e.g., Kuramoto oscillators, networks of which have been previously shown to approach synchronization exhibiting temporally varying patterns that are intrinsically related to the underlying connection topology [28]. The time-evolution to synchronization (i.e.,  $x_i = x$ ,  $y_i = y$ ,  $\forall i$ ) is analyzed using the pair-correlation function between oscillator phase angles  $\theta [= \arctan(y/x)]$ ,  $\rho_{ij}(t) = \langle \cos[\theta_i(t) - \theta_j(t)] \rangle$ , where  $\langle \dots \rangle$  is an average over random initial conditions. The fraction of synchronized nodes  $f_{sync}$  is obtained from the correlation matrix  $\rho$  by introducing a threshold. We observe that  $f_{sync}$  increases continuously to 1 (i.e., global synchronization) for WS networks. In contrast, the synchronization occurs over two distinct time-scales in modular random networks. At the relatively shorter time-scale of  $t_{ms}$ , local synchronization occurs among nodes belonging to the same module. Global synchronization occurs over a comparatively longer time-scale  $t_{gs}$ , with the synchronized clusters remaining fairly stable in the intervening time-period. Fig. 3(b) shows the variation of these two time-scales with  $r$ , converging when the network becomes homogeneous (as  $r \rightarrow 1$ ).

In the real world, for many systems the coupling strength between nodes within the same module may differ significantly from that between nodes belonging to different modules. For example, a recent study of tie strengths in mobile communication networks [29] observed that links connecting different communities tend to be weaker than links between members of the same com-

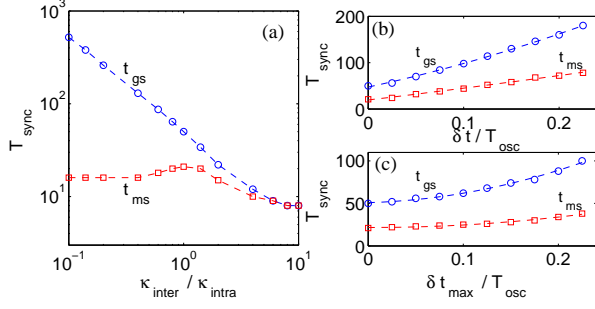


Fig. 4: (a) Dependence of the two time-scales corresponding to modular ( $t_{ms}$ ) and global synchronization ( $t_{gs}$ ) on the ratio of the inter and intra modular coupling strengths ( $\kappa_{inter}/\kappa_{intra}$ ). (b) The two synchronization time-scales shown as a function of a constant delay  $\delta t$  between any pair of connected oscillators. (c) Variation of  $t_{ms}$  and  $t_{gs}$  with random inter-modular coupling delays, that are distributed uniformly between  $[0, \delta t_{max}]$ . In this case, there is no delay for intra-modular couplings. Note that,  $T_{osc}$  is the time-period for an uncoupled relaxation oscillator. (In all cases  $N = 512$ ,  $\langle k \rangle = 14$ ,  $m = 16$  and  $r = 0.02$ ).

munity, supporting a well-known hypothesis for social networks [30]. Hence we look at the effect of different strengths for inter-modular coupling ( $\kappa_{inter}$ ) and intra-modular coupling ( $\kappa_{intra}$ ) on the synchronization behavior of oscillators on a modular network. As the inter-modular coupling strength becomes weaker relative to the intra-modular coupling, we observe the time-scales for modular and global synchronization to diverge (Fig. 4, a). Thus, in real systems where inter-community ties are relatively weaker, the time-scale separation between local and global events will be even more prominent. On the other hand, as the inter-modular coupling strength becomes large, the two time-scales gradually converge. As expected, at very large values of the ratio  $\kappa_{inter} : \kappa_{intra}$ , global and modular synchronization occur simultaneously.

We have also looked at the more general case of synchronization in the presence of delays in the coupling [31]. Even in the presence of delays, we observe distinct time-scales for modular and global events. If  $\delta t$  represents the delay period (i.e., the time required for signals to travel from one node to another through a link), the coupling terms of Eq (1) become:

$$\sum_{j=1}^N \frac{K_{ij}}{k_i} [x_j(t - \delta t) - x_i(t)]. \quad (3)$$

For constant delay (i.e.,  $\delta t = \text{constant}$ , for all pairs of connected nodes), we observe in Fig. 4 (b) that the time required for modular synchronization ( $\tau_{ms}$ ) is shorter than that required for global synchronization ( $\tau_{gs}$ ), although in general both are longer than their corresponding values in the absence of any delay ( $\delta t = 0$ ) considered earlier. We also consider the case where coupling delays are random and chosen from an uniform distribution. As in the case of

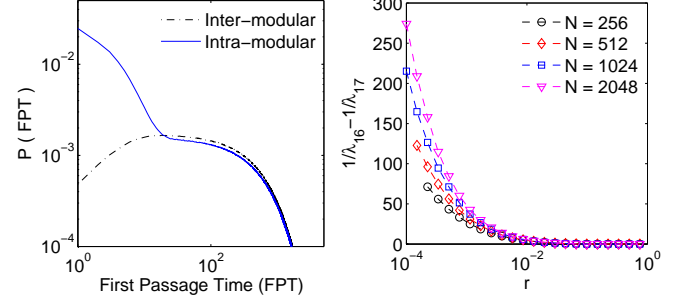


Fig. 5: (a) Distribution of first passage times (FPT) for diffusion process among nodes in a modular network ( $m = 16$ ,  $r = 0.02$ ,  $N = 512$ ,  $\langle k \rangle = 14$ ). The inter- and intra-modular FPTs indicate two distinct time-scales for random spreading, the process occurring much faster within a module than between modules. (b) The Laplacian spectral gap between the  $m$ -th and  $(m + 1)$ -th eigenvalues increases with decreasing  $r$ , shown for different system sizes with the number of modules  $m = 16$ .

coupling strengths  $\kappa$ , the delays may differ for connections between nodes belonging to the same module as opposed to those belonging to different modules. For example, this may arise if nodes within a module are geographically closer to each other, relative to nodes in other modules. Therefore, we look at the case when there is no coupling delay within a module, while, the delay for connections between oscillators in different modules is distributed over the interval  $[0, \delta t_{max}]$ . In Fig. 4 (c), we observe that as in the case of constant delay, the inter-modular synchronization takes significantly longer time than intra-modular synchronization, emphasising the generality of our results.

The existence of such distinct time-scales as a consequence of modular structure also appears in other dynamical processes, e.g., diffusion. Consider a discrete random walk on a network, where the walker moves from one node to a randomly chosen neighboring node at each time step. We analyze the time-evolution of the diffusion process by obtaining the distribution of first passage times for random walkers to reach a target node in the modular random network, starting from a source node [32]. Fig. 5(a) shows that this distribution differs quite significantly depending on whether the target node belongs to the same module as the source node or in a different module. This again suggests two distinct time-scales, with intra-modular diffusion occurring much faster than inter-modular diffusion. This is consistent with the results of Refs. [18, 33] where the degree of isolation of a module was assessed by comparing the participation of its nodes in different diffusion modes, using the internet as an example.

The occurrence of dynamical time-scale separation in modular networks can be understood analytically for diffusion and synchronization (under linear approximation) using a common framework. Although the oscillators we have considered are strongly non-linear, by linearizing the dynamics of the phase angle  $\theta$  around the synchro-

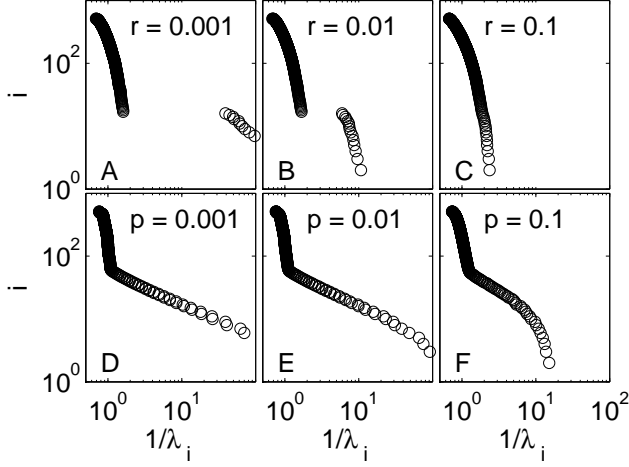


Fig. 6: Rank index  $i$  plotted against the inverse of the corresponding eigenvalue of the Laplacian matrix  $\mathcal{L}$  for modular random network ( $m = 16$ ) at different  $r$  (A-C) compared with that of WS network at different  $p$  (D-F), indicating the existence of a distinct spectral gap in the former at low  $r$  ( $N = 512$ ,  $\langle k \rangle = 14$ ).

nized state, their dynamics can be described as:  $\frac{d\theta_i}{dt} = -\frac{\kappa}{k_i} \sum_j L_{ij} \theta_j$ , where  $\mathbf{L}$  is the Laplacian matrix of the network, with  $L_{ii} = k_i$  and  $L_{ij} = -A_{ij}$  (for  $i \neq j$ ). The normal modes are  $\varphi_i(t) = \varphi_i(0) \exp(-\lambda_i t)$ , where  $\lambda_i$  are the eigenvalues of  $\mathbf{L}' = \mathbf{D}^{-1} \mathbf{L}$  ( $\mathbf{D}$  is a diagonal matrix with  $D_{ii} = k_i$ ). All the eigenvalues are real as  $\mathbf{L}'$  is related to the symmetric normalized Laplacian  $\mathcal{L} = \mathbf{D}^{\frac{1}{2}} \mathbf{L}' \mathbf{D}^{-\frac{1}{2}}$  through a similarity transformation. The mode corresponding to the smallest eigenvalue is associated with global synchronization, while other modes provide information about synchronization within different groups of oscillators. Difference in time-scales of the different modes is manifested as gaps in the spectrum of  $\mathcal{L}$ , which we indeed observe for modular random networks. The gap between modes corresponding to inter- and intra-modular synchronization increases with decreasing value of  $r$  [Fig. 5(b)]. Note that, the Laplacian spectra for WS networks does not exhibit a gap, indicating that the different time-scales for local and global synchronization originate from the modular organization (Fig. 6).

To relate this analysis with the diffusion process, we note that the transition probability from node  $i$  to  $j$  at each step of the random walk is  $P_{ij} = A_{ij}/k_i$ . This transition matrix  $\mathbf{P}$  is related to the normalized Laplacian of the network as  $\mathcal{L} = \mathbf{I} - \mathbf{D}^{\frac{1}{2}} \mathbf{P} \mathbf{D}^{-\frac{1}{2}}$ , where  $\mathbf{I}$  is the identity matrix [18]. The eigenvalues of  $\mathbf{P}$  are all real, the largest being 1 while the others are related to the different diffusion time-scales. As in the synchronization example, the spectrum of  $\mathbf{P}$  for modular random network exhibits a gap reflecting the existence of distinct time-scales in the system. Note that, although the above result strictly applies only when linear approximation is valid, we observe

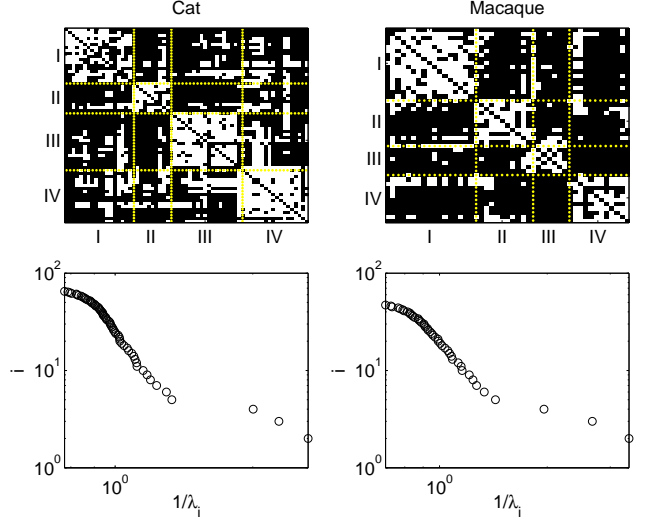


Fig. 7: The adjacency matrix showing connections between different cortical areas in the cat (top left,  $N = 65$ ) and macaque (top right,  $N = 47$ ) cerebral cortex. The broken lines indicate clusters of cortical areas (labelled I-IV) that are densely connected within themselves. This structural division reflects, to some extent, the functional segregation among the different cortical areas (e.g., visual, somatosensory, etc.). The rank-ordered reciprocal eigenvalues of the corresponding Laplacian matrices (bottom) show well-defined spectral gaps, consistent with the existence of a modular structure for the cortico-cortical networks. The multiple gaps indicate that synchronization between different modules occur at different times.

the property of time-scale separation predicted for modular networks to be a much more general phenomenon. In particular, the strong nonlinear interactions of the Ising model cannot be even approximately treated by the Laplacian analysis. Nevertheless, we see almost identical behavior for all three processes, indicating the universality of the dynamical signature of modular networks.

The above distinction between the dynamical behavior for different SWN models can be empirically tested by considering the cortico-cortical networks in the brains of cat [34] and macaque [35] which have been reported to possess clustered small-world properties [8]. Fig. 7 shows the existence of gaps in the Laplacian spectra of these networks, suggesting a modular organization of the connections between the cortical areas. This is consistent with the fact that local synchronization within a cluster has functional importance in the brain, whereas global coherence of activity may be undesirable. This example suggests that at least some of the SWN reported in nature may have modular organization with significantly different dynamical behavior from the WS or related models.

In this paper, we have shown that modular networks, although they exhibit all the structural features associated with SWN, have the striking feature of multiple discrete time-scales, in contrast to WS and related models. As



dynamics at the local and global levels may have different consequences in most natural systems, the temporal separation between processes occurring at distinct scales through modular organization underlines the importance of such network structures. We suggest that this facilitation of time-scale separation could be the reason for the ubiquity of modularity in real-world networks, where it can emerge through multi-constraint optimization [36]. It is being increasingly recognized that SWN mediate processes of critical importance to society, including the spreading of epidemics such as SARS [37]. To prevent an initially local perturbation from rapidly spreading and evolving into a global threat requires an intelligent intervention strategy that should take into account the underlying network structure, such as modules, which governs the collective dynamics of the system.

\* \* \*

We would like to thank R. Anishetty, D. Dhar, G. Menon, R. Rajesh and S. Sinha for helpful discussions.

## REFERENCES

- [1] GRAY C. M., KONIG P., ENGEL A. K. and SINGER W., *Nature* , **338** (1989) 334.
- [2] KANDEL E. R., SCHWARTZ J. H. and JESSELL T. M., *Principles of Neural Science* 4th Edition (McGraw-Hill, New York) 2000.
- [3] STROGATZ S. H., *Nature* , **410** (2001) 268.
- [4] WATTS D. J. and STROGATZ S. H., *Nature* , **393** (1998) 440.
- [5] DOROGOVTSSEV S. and MENDES J., , **cond-mat/0404593** (.)
- [6] NEWMAN M. E. J., *SIAM Review* , **45** (2003) 167.
- [7] EGUÍLUZ V. M., CHIALVO D. R., CECCHI G. A., BALIKI M. and APKARIAN A. V., *Phys. Rev. Lett.* , **94** (2005) 018102.
- [8] BASSETT D. S. and BULLMORE E., *Neuroscientist* , **12** (2006) 512.
- [9] HUMPHRIES M. D., GURNEY K. and PRESCOTT T. J., *Proc. Roy. Soc. London, Ser. B* , **273** (2006) 503.
- [10] NEWMAN M. E. J., WATTS D. J. and STROGATZ S. H., *Proc. Natl. Acad. Sci. U.S.A.* , **99** (2002) 2566.
- [11] FELL D. A. and WAGNER A., *Nat Biotechnology* , **18** (2000) 1121.
- [12] JEONG H., TOMBER B., ALBERT R., OLTVAI Z. and BARABASI A.-L., *Nature* , **407** (2000) 651.
- [13] NEWMAN M. E. J., *J. Stat. Phys.* , **101** (2000) 819.
- [14] HARTWELL L. H., HOPFIELD J. J., LEIBLER S. and MURRAY A. W., *Nature* , **402** (1999) C47.
- [15] GUIMERA R. and AMARAL L. A. N., *Nature* , **433** (2005) 895.
- [16] HOLME P., HUSS M. and JEONG H., *Bioinformatics* , **19** (2003) 532.
- [17] ARENAS A., DANON L., DIAZ-GUILERA A., GLEISER P. M. and GUIMERA R., *Eur. Phys. J. B* , **38** (2004) 373.
- [18] ERIKSEN K. A., SIMONSEN I., MASLOV S. and SNEPPEN K., *Phys. Rev. Lett.* , **90** (2003) 148701.
- [19] KRAUSE A. E., FRANK K. A., MASON D. M., ULANOWICZ R. U. and TAYLOR W. W., *Nature* , **426** (2003) 282.
- [20] GIRVAN M. and NEWMAN M. E. J., *Proc. Natl. Acad. Sci. U.S.A.* , **99** (2002) 7821.
- [21] LATORA V. and MARCHIORI M., *Phys. Rev. Lett.* , **87** (2001) 198701.
- [22] NEWMAN M. E. J. and GIRVAN M., *Phys. Rev. E* , **69** (2004) 026113.
- [23] DERENYI I., PALLA G. and VICSEK T., *Phys. Rev. Lett.* , **94** (2005) 160202.
- [24] BOCCALETTI S., LATORA V., MORENO Y., CHAVEZ M. and HWANG D.-U., *Physics Reports* , **424** (2006) 175.
- [25] VALENTE T. W., *Network Models of the Diffusion of Innovations* (Hampton Press, Cresskill, NJ) 1995.
- [26] PASTOR-SATORRAS R. and VESPIGNANI A., *Phys. Rev. Lett.* , **86** (2001) 3200.
- [27] CASTELLO X., TOIVONEN R., EGUILUZ V. M., SARAMAKI J., KASKI K. and MIGUEL M. S., *Europhys. Lett.* , **79** (2007) 66006.
- [28] ARENAS A., DIAZ-GUILERA A. and PEREZ-VICENTE C. J., *Phys. Rev. Lett.* , **96** (2006) 114102.
- [29] ONNELA J. P., SARAMAKI J., HYVONEN J., SZABO G., LAZER D., KASKI K., KERTESZ J. and BARABASI A. L., *Proc. Natl. Acad. Sci. U.S.A.* , **104** (2007) 7332.
- [30] GRANOVETTER M., *Am. J. Soc.* , **78** (1973) 1360.
- [31] ARENAS A., DIAZ-GUILERA A., KURTHS J., MORENO Y. and ZHOU C., *Phys. Rep.* , **469** (2008) 93.
- [32] BARONCHELLI A. and LORETO V., *Phys. Rev. E* , **73** (2006) 026103.
- [33] MASLOV S., SNEPPEN K. and ZALIZNYAK A., *Physica A* , **333** (2003) 529.
- [34] SCANNELL J. W., BLAKEMORE C. and YOUNG M. P., *J. Neuroscience* , **15** (1995) 1463.
- [35] HONEY C. J., KOTTER R., BREAKSPEAR M. and SPORNS O., *Proc. Natl. Acad. Sci. U.S.A.* , **104** (2007) 10240.
- [36] PAN R. K. and SINHA S., *Phys. Rev. E* , **76** (2007) 045103.
- [37] COLIZZA V., BARRAT A., BARTHELEMY M. and VESPIGNANI A., *BMC Med.* , **5** (2007) 34.